

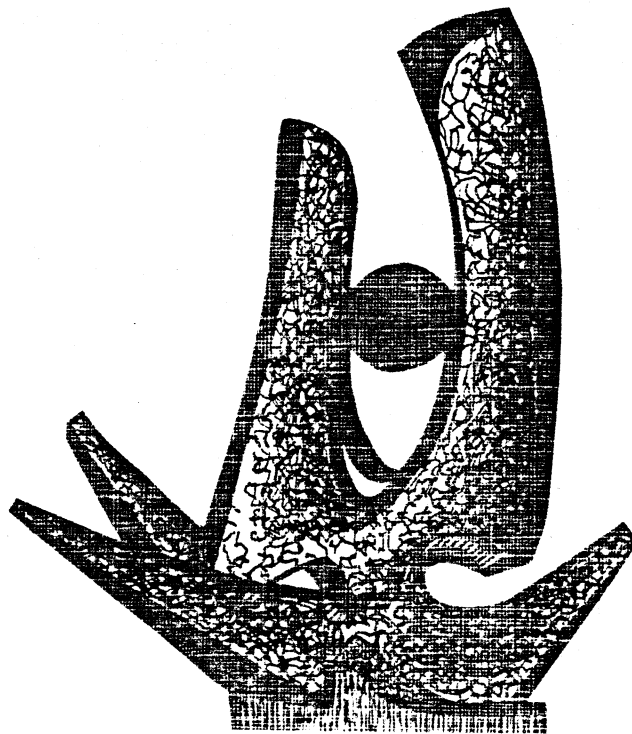
MICHIGAN STATE UNIVERSITY

CYCLOTRON LABORATORY

NEW RESULTS AT INTERMEDIATE ENERGIES

C.K. GELBKE

Invited talk given at the  
International Conference on Nucleus-Nucleus Collisions  
held at East Lansing, September 27-October 1, 1982



SEPTEMBER 1982

1/20/2000

—



NEW RESULTS AT INTERMEDIATE ENERGIES

C.K. Gelbke\*

Department of Physics and  
National Superconducting Cyclotron Laboratory  
Michigan State University  
East Lansing, MI 48824, USA

**Abstract:** Recent experimental results on light particle emission from intermediate energy nucleus-nucleus collisions are reviewed. Present, mostly single particle inclusive measurements are consistent with the concept of thermalization of a subset of nucleons. The measurement of thermally produced composite light particles is hoped to provide more specific information about the decay properties of hot nuclear matter and a possible liquid gas phase transition.

I. Introduction

Over the last few decades, nuclear physics had its major focus on detailed spectroscopic studies of nuclei at low excitation energies, generally not exceeding a few tens of MeV. The availability of nuclear projectiles covering a large range of mass and energy provides a unique opportunity to explore the statistical and dynamical properties of strongly interacting many body systems at considerably higher excitation energies. Efforts to investigate the global properties of hot and dense nuclear matter present a marked deviation from the more traditional field of nuclear spectroscopy. It has become clear, by now, that this exciting task will be quite difficult - both from the experimental and the theoretical points of view.

Little is known about the thermodynamic properties of nuclear matter, except for the binding energy ( $E_B \approx 16$  MeV) and incompressibility ( $K \approx 210$  MeV) at normal nuclear density ( $\rho_0 \approx 0.15$  fm<sup>-3</sup>). Experiments in the laboratory are confined to small ensembles of nucleons ( $A \leq 500$ ). Even if highly excited states of statistical equilibrium can be achieved for such ensembles, they would immediately decay by particle emission due to the large surface area. Inferences about the thermodynamic properties of nuclear matter, therefore, have to rely on a solid understanding of these decay processes.

Up to now, the decay of statistical nuclear ensembles by particle emission has mainly been treated in two extremes. For low energy nuclear reactions, the decay of the compound nucleus can be quantitatively understood in terms of the Hauser-Feshbach theory<sup>1)</sup>. This theory corresponds to particle evaporation from the liquid phase of nuclear matter. Thermodynamic approaches at higher energies<sup>2-4)</sup>, on the other hand, have been based on the assumption of an expanding gas of nuclear matter in thermodynamic equilibrium. The equilibrium distribution of this hot nuclear gas is then assumed to be "frozen" out, once the density has decreased to the freeze-out density  $\rho_f$ , below which collisions between the gas constituents become negligible.

It is only recently, that the possible coexistence of the gas

\*Alfred P. Sloan Fellow

and liquid phases has been taken into consideration<sup>5-7</sup>). Figure 1 shows a pressure versus density diagram calculated for nuclear matter with a Skyrme-type interaction<sup>6</sup>). For temperatures lower than the critical temperature  $T_c \approx 20$  MeV, the liquid and gaseous phases coexist over a certain range of density (see hatched area in Figure 1). At the critical temperature, liquid and gas phases can only coexist at the critical density  $\rho_c \approx 0.07 \text{ fm}^{-3}$ . At higher temperatures only the gas phase exists.

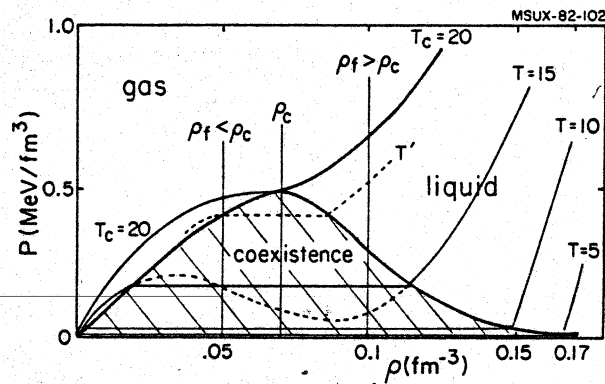


Figure 1: Diagram of pressure versus density for nuclear matter as calculated<sup>6</sup>) with a Skyrme - type interaction. The regions corresponding to the liquid and gas phases as well as the region of coexistence of the two phases are indicated.

If the freeze-out density  $\rho_f$  is larger than the critical density  $\rho_c$ , the equilibrium distribution will contain a certain amount of nuclear matter in the liquid phase, corresponding to bound clusters, as long as the freeze-out temperature  $T_f$  is lower than the critical temperature  $T_c$ . For  $T_f > T_c$ , on the other hand, the liquid phase vanishes and a drastic reduction of complex particle production should be observed experimentally. For  $\rho_f < \rho_c$  and for  $T < T_c$ , the system may enter the purely gaseous phase while still in the equilibrium expansion stage leading to a possible uncertainty in the experimental determination of  $T_c$ . For  $\rho_f \lesssim 0.4 \rho_c$ , this uncertainty should be of the order of 1 MeV (see ref. 6 for more details).

Obviously, the experimental determination of the critical temperature and the observation of the phase instability at the point  $(T_c, \rho_c)$  would be of great interest. As the foregoing simple arguments suggest such a program would encompass measuring the temperature dependence of the relative abundance of nucleons and composite particles. At the same time, it should be clear that the above arguments have been made for infinite nuclear matter in thermodynamic equilibrium and will have to be extended to the more realistic case of finite nuclear systems.

In the meantime, first explorative experiments have been performed and some qualitative trends are beginning to emerge from the experimental data. In this talk, I will discuss the energy dependence of intermediate rapidity nucleon and composite light particle emission in nuclear collisions between light projectile nuclei ( $A \approx$

-20) and heavy target nuclei ( $A \approx 200$ ). I would like to stress at the onset that my approach will be rather schematic. Instead of trying to do justice to the entire complexity of intermediate energy nucleus - nucleus collisions, I will use certain simplifying assumptions that make it possible to describe a large body of data in terms of a few parameters. These parameters can then be compared to simple model calculations revealing some relevant effects that should be incorporated into more sophisticated analyses of the future.

## 2. Energy Spectra: The Assumption of Local Equilibrium

Light particle emission in low energy nucleus-nucleus collisions ( $E/A \leq 5$  MeV) occurs predominantly after full statistical equilibrium of all intrinsic degrees of freedom has been attained by the primary reaction products. In this case, the decay of the primary reaction products can be well understood in terms of the Hauser-Feshbach theory of compound nucleus decay. With increasing energy, light particle emission prior to the attainment of full statistical equilibrium becomes important. As an example, Figure 2 shows the neutron spectra measured<sup>8</sup>) for  $^{16}\text{O}$  induced reactions on  $^{238}\text{U}$  at  $E/A = 19.4$  MeV. Neutrons emitted at low energies originate primarily from fully equilibrated nuclei (as shown by the dashed lines in Figure 2) whereas the emission of high-energy neutrons occurs primarily prior to the attainment of full statistical equilibrium (as shown by the solid lines in Figure 2). For the  $^{16}\text{O} + ^{238}\text{U}$  reaction, the deexcitation of the fully equilibrated heavy reaction products (compound nucleus or fission fragments) occurs primarily via neutron emission. For charged particle emission, the equilibrium component is, therefore, strongly reduced in magnitude as compared to the non-equilibrium component.<sup>9</sup>)

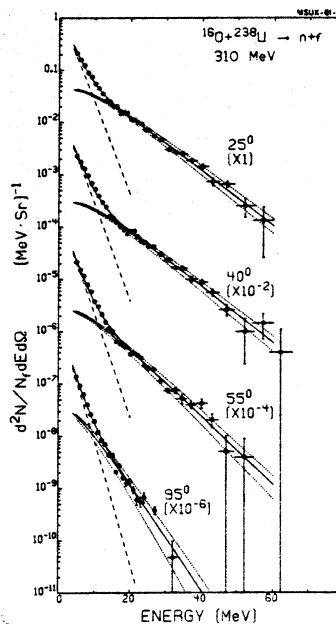


Figure 2: Differential neutron multiplicities per fission event measured for the reaction  $^{238}\text{U}(^{16}\text{O},\text{nf})$  at 310 MeV. The solid and dashed lines show the decomposition into equilibrium and non-equilibrium components, respectively<sup>8</sup>).

Originally, the non-equilibrium components of the light particle spectra were associated with the rather trivial processes of projectile breakup or statistical decay of excited projectile residues. Only by demonstrating the fusion of nearly the entire projectile with the target nucleus (and thereby eliminating contributions from decaying projectile residues) has non-equilibrium light particle emission been established beyond doubt.

The experimental technique that has been employed<sup>9,10</sup>) for the  $^{16}\text{O} + ^{238}\text{U}$  reaction is illustrated in Figure 3. For fissionable

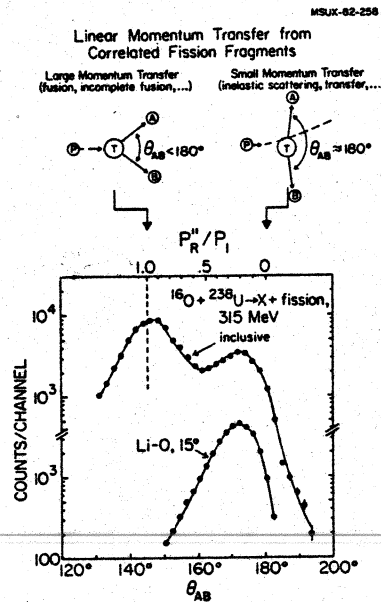


Figure 3: Folding angle distributions observed<sup>9,10</sup>) for  $^{16}\text{O}$  induced reactions on  $^{238}\text{U}$  at 310 MeV.

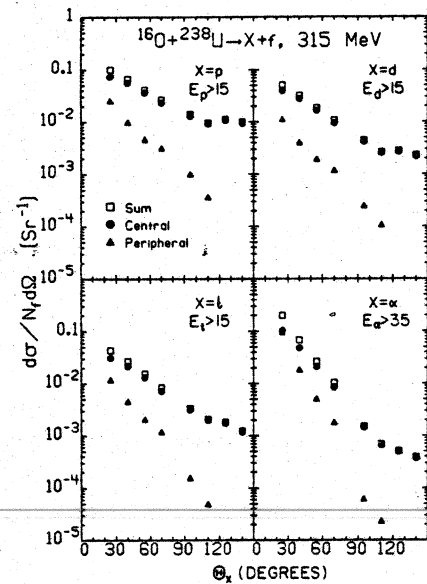


Figure 4: Angular distributions of protons, deuterons, tritons and alpha particles measured for fusion-like ("central",  $p_R''/p \geq 0.5$ ) and transfer-like ("peripheral",  $p_R''/p \leq 0.5$ ) collisions.<sup>9</sup>)

target nuclei, information about the linear momentum transfer to the target residue may be obtained by measuring the folding angle  $\theta_{AB}$  between the two fission fragments resulting from the decay of the target residue. Increasing linear momentum transfers correspond to smaller folding angles. By means of this technique it is possible to distinguish "central" or fusion-like reactions from "peripheral" or transfer-like reactions (for which sequential decay processes may be important). The angular distribution of energetic protons, deuterons, tritons and alpha particles observed<sup>9</sup>) in "central" and "peripheral" collisions are shown in Figure 4. At forward angles, both processes contribute. With increasing detection angle of the coincident light particle, the relative contribution of transfer-

like "peripheral" collisions decreases rapidly as compared to the contribution from fusion-like "central" collisions. Except at very forward angles, the cross section for non-equilibrium light particle emission is dominated by fusion-like reactions.

Qualitatively similar conclusions were arrived at<sup>11)</sup> for  $^{16}\text{O}$  induced reactions at  $E/A = 100$  MeV. Figure 5 shows the target dependence of the energy integrated proton cross sections measured at various laboratory angles. At forward angles these cross sections vary as  $A^{1/3}$  and at larger angles they vary as  $A^{2/3}$ , indicating that forward angle proton emission is dominated by peripheral collisions whereas proton emission at larger angles is dominated by more central collisions.

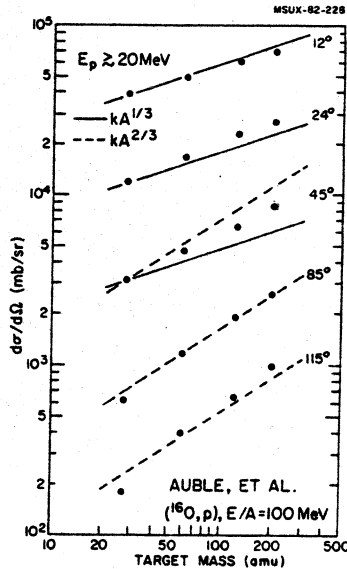


Figure 5: Target dependence of energy-integrated yields of protons produced in  $^{16}\text{O}$  induced reactions<sup>11)</sup> at  $E/A = 100$  MeV.

With the exception of the most forward and backward angles, the emission of light particles can be rather well described in terms of a Maxwellian distribution centered about a velocity that is, in general, slightly less than half the beam velocity. In the laboratory rest frame, the invariant cross section is given by<sup>9,12)</sup>

$$\frac{E_0}{p} \frac{d^2\sigma}{dpd\Omega} = \frac{1}{p} \frac{d^2\sigma}{dE_0 d\Omega} = CY(E_0 - \beta p \cos \theta) \exp \left\{ - \gamma (E_0 - \beta p \cos \theta) / T \right\} \quad (1)$$

where  $\beta$  is the source velocity,  $p$  is the laboratory momentum of the particle of rest mass  $m_0$ ,  $\gamma = (1 - \beta^2)^{-1/2}$  and  $E_0 = (p^2 + m_0^2)^{1/2}$ . The normalization is given by

$$C = \frac{\sigma_0}{4\pi m_0^3} \left[ 2(T/m_0)^2 K_1(m_0/T) + (T/m_0) K_0(m_0/T) \right]^{-1}, \quad (2)$$

where  $\sigma_0$  is the cross section, and  $K_0$  and  $K_1$  are MacDonal functions. Non-relativistically, the cross sections can be expressed as

$$\frac{d^2\sigma}{dE d\Omega} = \frac{\sigma_0}{2(\pi T)^{3/2}} E^{3/2} \exp \left\{ -(E+E_1 - 2E^{1/2}E_1^{1/2} \cos \theta)/T \right\}, \quad (3)$$

Where  $E = p^2/2m$  is the kinetic energy and  $E = m\beta^2/2$ . The Coulomb repulsion from a stationary target nucleus can be approximated<sup>9,13)</sup> by replacing  $E$  with  $E - E_c$ , where  $E_c$  is the kinetic energy gained by the light particle due to the Coulomb repulsion from the target.

Using this simple moving source parameterization a rather large set of inclusive light particle production cross sections can be described.<sup>11-13)</sup> As an example, Figure 6 shows the inclusive proton energy spectra measured<sup>13)</sup> for  $^{16}\text{O}$  induced reactions on  $^{197}\text{Au}$  at  $E/A = 13.4$  and  $19.4$  MeV. Except at the most forward angles, the moving source parameterization describes the data quite satisfactorily. At this point, it should be absolutely clear that this parameterization is not consistent with evaporation from the compound nucleus (which cannot explain these data<sup>13)</sup> but corresponds rather to the achievement of thermal equilibrium for a subset of nucleons.

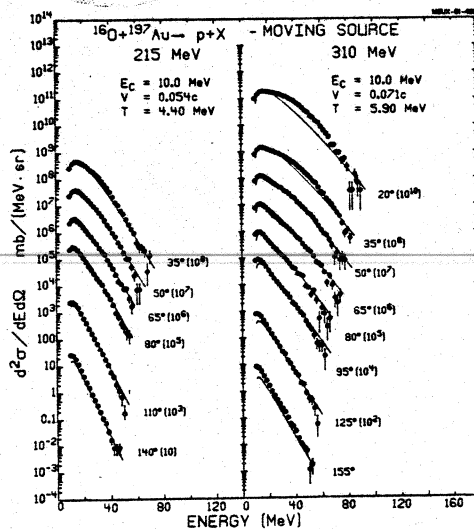


Figure 6: Energy spectra measured for the reaction  $^{16}\text{O} + ^{197}\text{Au} \rightarrow p + X$  at  $E/A = 13.4$  and  $19.4$  MeV. The solid lines are fit to the data with the moving source parameterization including the effect of Coulomb repulsion from the target residue.<sup>13)</sup>

The assumption of thermal equilibrium for a subset of nucleons implies that the emission of coincident light particles should be dynamically uncorrelated. In Figure 7, proton energy spectra are compared that were measured<sup>14)</sup> in single- and two-proton inclusive experiments for  $^{16}\text{O}$  induced reactions on Al and Au targets at  $E/A = 19.4$  MeV. Within the statistical accuracy of these measurements, the shapes of light particle energy spectra observed in coincidence with a second light particle were found to be very similar to the shapes of the singles energy spectra. In fact, the observed correlations between two coincident light particles were of comparable order of magnitude as the ones imposed on finite nucleon ensembles by energy and momentum conservation, indicating that the assumption of statistical



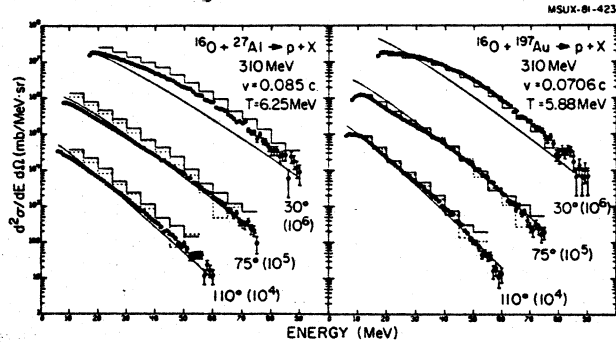


Figure 7: Comparison of single-proton (solid points) and two-proton (histograms) inclusive energy spectra measured<sup>14)</sup> for  $^{16}\text{O}$  induced reactions on Al and Au at  $E/A = 19.4$  MeV. The solid histograms show the energy spectra measured when a coincident proton is detected at the angle of  $\theta = -30^\circ$  on the opposite side of the beam axis and the dashed histograms show the energy spectra measured when the coincident proton is detected at  $\theta = +30^\circ$  at the same side of the beam axis. The solid curves are the energy spectra calculated with the moving source parameterization.

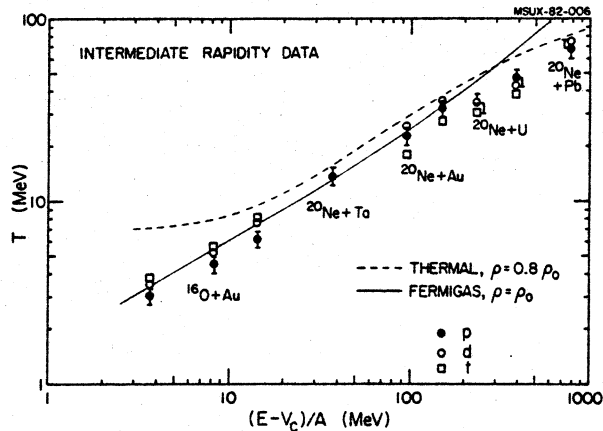


Figure 8: Energy dependence of temperature parameter  $T$  extracted<sup>12)</sup> from moving source fits to light particle spectra measured for  $^{16}\text{O}$  and  $^{20, 22}\text{Ne}$  induced reactions on heavy targets. The curves shown in the figure are discussed in the text.

equilibrium of a subset of nucleons is not strongly violated.<sup>14)</sup>

Figure 8 shows the dependence of the temperature parameter  $T$  that has been extracted<sup>12)</sup> from similar fits to light particle spectra in  $^{16}\text{O}$  and  $^{20, 22}\text{Ne}$  induced reactions on heavy targets over a wide range of projectile energies. To minimize contributions from peripheral processes such as knock-out reactions or projectile break-up and sequential decay, only those light particles were included in the analysis<sup>12)</sup> that were emitted at laboratory angles larger than

-50° and with energies above the ones expected from compound nucleus evaporation. The data thus selected will be loosely referred to as "intermediate rapidity data". Most certainly, this approach involves a certain degree of arbitrariness and makes the discussion somewhat model dependent. It allows, however, to delineate some systematic trends that emerge from existing data. Note, that rather similar temperature parameters are obtained for different light particle species produced via the same entrance channel - consistent with the assumption of local thermal equilibrium. The solid curve shown in the figure corresponds to the temperature of a Fermigas of normal nuclear density consisting of equal numbers of target and projectile nucleons. Except for the highest energies, where cooling by pion production is expected to become important, this curve follows the trend of the data rather well. For comparison, the dashed line corresponds to calculations for a free, strongly-interacting gas in thermal and chemical equilibrium as predicted by the fireball model<sup>15,16</sup>) for the impact parameters of maximum weight assuming a freeze-out density of  $\rho_f = 0.8 \rho_0 = 0.12 \text{ fm}^{-3}$ . In the following, these calculations will be termed simply "fireball model calculations." (It should be realized, however, that the geometrical aspect of impact parameter averaging of the original fireball model has been omitted for the purpose of simplicity.) These calculations are in better agreement with the data at higher energies than the simple Fermi-gas estimate but disagree with the data at the lower energies where, most likely, the assumption of a free gas is not correct and the liquid phase has to be taken into account; see Figure 1 for orientation.

### 3. Composite Particles: The Assumption of Statistical Emission from the Liquid and Gas Phases

Up to now we have discussed the shapes of light particle energy spectra in terms of the temperature parameter  $T$ . We now discuss the magnitude of the intermediate rapidity light particle cross sections and the relative abundance of nucleons and composite light particles in terms of the parameter  $\sigma$ , see eqs. 1-3.

The intermediate rapidity light particle cross sections extracted from fits to the data with the moving source parameterization are shown in Figure 9. The cross sections for the emission of hydrogen isotopes increase by more than two orders of magnitude for energies per nucleon above the Coulomb barrier ranging from 4 to 800 MeV. At the highest energies, the cross sections are close to the ones expected from the participant - spectator model. The dot-dashed curve shows the energy dependence of the proton cross sections calculated with the fireball model.<sup>17</sup>) These calculations reflect the predicted temperature dependence of the chemistry of a free, strongly-interacting gas; with increasing temperature the formation of composite light particles becomes less probable, leading to a modest increase of the proton yield with increasing energy. It is clear that the model cannot explain the dramatic variation of the cross sections with energy that is observed experimentally. This is, perhaps, not too surprising, since the participant spectator model is expected to break down at lower energies: the participants are not likely to form a free gas and the liquid phase will probably have to be taken into account.

It can already be seen from Figure 9, that the cross sections for intermediate energy protons, deuterons and tritons exhibit rather similar energy dependences whereas the energy dependence of alpha

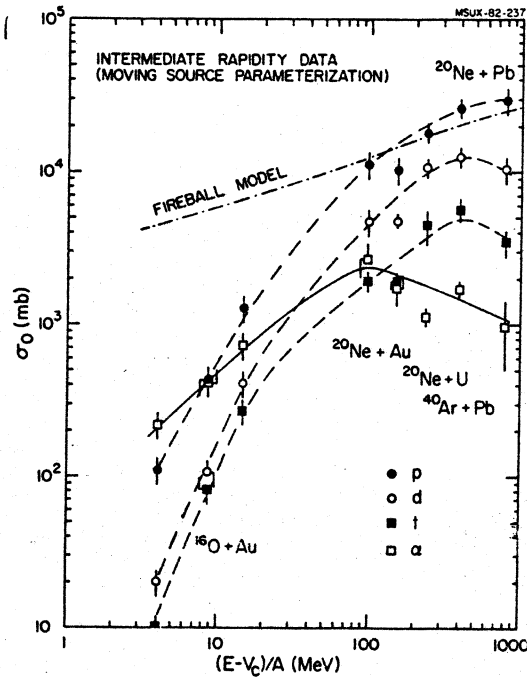


Figure 9: Energy dependence of intermediate rapidity light particle cross sections determined<sup>12)</sup> from moving source fits. The solid and dashed curves are drawn to guide the eye. The dot-dashed curve labelled "fireball model" represents the energy dependence of the proton yield predicted for a free, strongly-interacting gas.<sup>17)</sup>

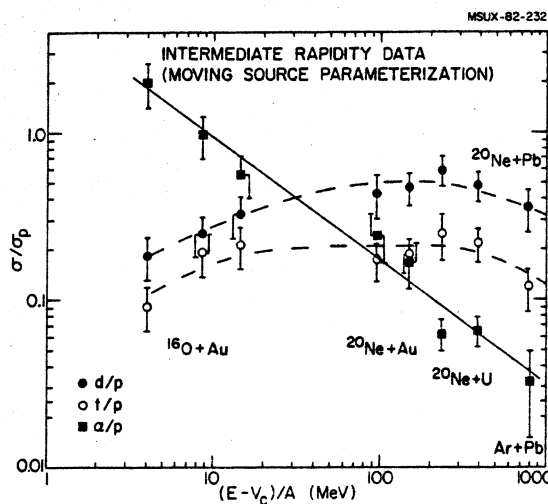


Figure 10: Ratio of composite light particle to proton yields determined<sup>12)</sup> from moving source fits.

particle cross sections is markedly different. This is more clearly demonstrated in Figure 10 where the ratio of composite light particle and proton cross sections is displayed. The relative abundance of the three hydrogen isotopes p, d, and t depends only slightly on

energy. The cross section ratios  $\sigma_\alpha/\sigma_p$  and  $\sigma_t/\sigma_p$  vary by less than a factor of three and appear to exhibit very broad maxima as a function of projectile energy. The relative abundance of protons and alpha particles, on the other hand, exhibits a rather strong energy dependence. The ratio  $\sigma_\alpha/\sigma_p$  decreases by more than 1½ orders of magnitude over the energy range under consideration. This rather dramatic decrease of  $\sigma_\alpha/\sigma_p$  with incident projectile energy has been interpreted<sup>6,7)</sup> in terms of a liquid-gas phase transition at the critical temperature  $T_c \approx 20$  MeV.

It is probably fair to say that we do not yet have a sufficiently detailed understanding of composite light particle production mechanisms to rule out alternative interpretations. In the following I want to discuss some characteristic features of two extreme models corresponding to statistical particle emission from the gaseous and liquid phases.

The assumption of thermal and chemical equilibrium for a free, strongly-interacting nuclear gas<sup>2-4,15,16)</sup> has been applied rather successfully to the interpretation of high-energy nucleus-nucleus collisions. In order to isolate the characteristic thermodynamic features of particle emission from an equilibrated gas from the geometrical aspects of the reaction (which mainly determine the overall magnitude of the cross sections) we will restrict our consideration to the cross section ratios  $\sigma/\sigma_p$  of composite light particles and protons.

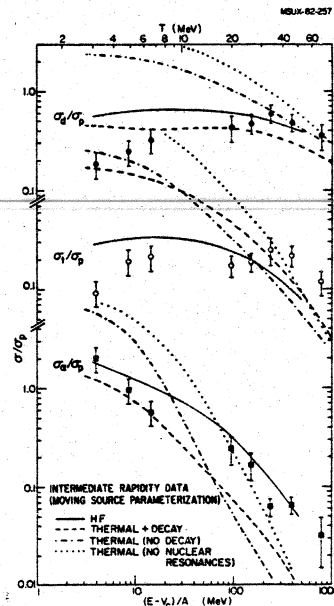


Figure 11: Comparison of composite particle to proton yield ratios with various model calculations. The dotted curves correspond to thermal calculations<sup>1)</sup> for a free, strongly-interacting gas that exclude the formation of nuclear resonances; the dot-dashed curves represent calculations that include the formation of nuclear resonances but exclude their decay products after freeze-out; the dashed curves correspond to calculations that include the contribution from the decay of nuclear resonances after freeze-out<sup>17)</sup> as is done in the fireball model calculations. The solid lines correspond to the Hauser-Feshbach type calculations of Friedman and Lynch.<sup>18,19)</sup>

The dashed curves shown in Figure 11 correspond to our (simplified) fireball model calculation<sup>17)</sup> which includes the entire thermodynamics of the original fireball model<sup>15,16)</sup> and the more elaborate firestreak model<sup>4)</sup>. The calculations include the formation of

nuclear resonances and the contribution of their decay after freeze-out to the p, t and  $\alpha$  cross sections whereas it is assumed that no nuclear resonances decay to deuterons. These calculations approximately reproduce the observed  $\sigma_d/\sigma_p$  and  $\sigma_\alpha/\sigma_p$  ratios but completely fail to reproduce the energy dependence of the observed  $\sigma_t/\sigma_p$  ratios. It should be realized that the predicted  $\sigma_t/\sigma_p$  ratio is of the right order of magnitude at high energies where the assumption of a free gas is best justified. The failure of the model calculation occurs primarily for the lower energies where the assumption of a free gas in thermal equilibrium is probably not a good approximation. If this explanation is correct, the approximate agreement of these calculations with the experimental trends of the  $\sigma_d/\sigma_p$  and  $\sigma_\alpha/\sigma_p$  ratios will have to be questioned and might be fortuitous.

The partial success of the fireball model calculations and, perhaps more importantly, the partial failure of these calculations make it of interest to consider the qualitative effects of some of the ingredients that have been incorporated into these calculations. The dot-dashed curves in Figure 11 correspond to fireball model calculations that exclude the decay of nuclear resonances into observed particles after freeze-out. This (unrealistic) calculation fails completely to reproduce the experimental observations. It does, however, demonstrate the outstanding importance of these decay processes within the framework of this model - particularly at low energies. In this model, the formation of composite particles and particle unstable nuclear resonances becomes increasingly important at lower energies. Many of these resonances decay by proton emission, but not by deuteron emission. This causes a decrease of the final  $\sigma_d/\sigma_p$  ratio as compared to the one existing at freeze-out.

Finally, it should be pointed out that the inclusion of nuclear resonances into the thermodynamics of the fireball is absolutely essential. To demonstrate this fact the dotted curves of Figure 11 show calculations in which the existence of particle unbound nuclear resonances is entirely neglected. The disagreement with the data has become even worse for these calculations. The importance of nuclear resonances for the fireball chemistry implies that any theory of light particle production will have to take the effects of sequential decay of particle unstable states into consideration; this, unfortunately, adds to the difficulties of correctly interpreting the experimental data.

The deexcitation of nuclei at low excitation energies can be rather well understood in terms of the Hauser-Feshbach theory of compound nucleus decay. With increasing excitation energy nuclear shell effects will wash out and the Hauser-Feshbach theory can be extended to the case of statistical particle emission from an excited liquid drop of nuclear matter.<sup>18)</sup> The present formulation<sup>18)</sup> of Friedman and Lynch is based on the assumption of global thermal equilibrium for the entire liquid drop. Present experimental evidence, on the other hand, indicates that thermal equilibrium is only obtained for a subset of nucleons. The quantitative treatment of nucleon and composite particle emission from a liquid drop of nuclear matter for which only local thermal equilibrium has been attained presents an interesting subject for future theoretical work. On the other hand, it is very instructive and consistent with the somewhat schematic approach of this talk to consider the simplified case of particle emission from a hot liquid drop of nuclear matter which will be characterized by its initial temperature T, mass number A and charge number Z. The decay properties of such a liquid drop are expected to vary rather smoothly with A and Z. For fixed A/Z ratio, the size of the liquid drop should primarily affect

the total number of particles evaporated from the drop. For simplicity we will choose  $A = 217$ ,  $Z = 89$  and multiply the number of evaporated particles with an energy independent normalization constant  $\sigma_0$ .

The rate of emission of particle X composed of  $Z_x$  protons and  $N_x$  neutrons from a liquid drop of nuclear matter at constant density is given by<sup>18)</sup>

$$\frac{dN_x}{dE dt} = C_x (E - V_x) \cdot \theta(E - V_x) \times \exp \left\{ -\frac{1}{T} \left[ E + B_x - Z_x f(T, \rho_z) - N_x f(T, \rho_n) \right] \right\}, \quad (4)$$

where

$$C_x = (2S_x + 1) \frac{M_x R_x^2}{\pi \hbar^3}. \quad (5)$$

Here,  $S_x$ ,  $m_x$ ,  $V_x$  and  $B_x$  are the spin, mass, Coulomb barrier and separation energy of particle X. The radius  $R_x$  is defined in terms of the geometrical cross section for the inverse capture reaction,  $\pi R_x^2$ . The function  $\theta(E)$  is unity for positive argument and zero otherwise. The free excitation energies per nucleon for the charged and neutral components of densities  $\rho_z$  and  $\rho_n$  are denoted by  $f(T, \rho_z)$  and  $f(T, \rho_n)$  where,  $f(T, \rho) = \epsilon^*(T, \rho) - T \sigma(T, \rho)$  and  $\epsilon^*$  and  $\sigma$  are the excitation energy per particle and the entropy per particle.

Integration of eq. (4) over energy yields

$$\frac{dN_x}{dt} = C_x T^2 \exp \left\{ -\frac{1}{T} \left[ V_x + B_x - Z_x f(T, \rho_z) - N_x f(T, \rho_n) \right] \right\}. \quad (6)$$

Using the low temperature limit of a fermi gas for the free energy

$$f(T, \rho) \approx -\frac{\pi^2}{4\epsilon_F} T^2, \quad (7)$$

one obtains for the branching ratios

$$\frac{\Gamma_x}{\Gamma_p} \approx \frac{C_x}{C_p} \exp \left\{ \frac{Q_x}{T} - \frac{(A_x - 1) \pi^2 T}{4\epsilon_F} \right\} \quad (8)$$

where

$$Q_x = B_p + V_p - B_x - V_x \quad (9)$$

Friedman and Lynch have written a computer program<sup>18)</sup> that calculates the entire history of particle emission from a hot liquid drop as it cools down, including the emission of particle unstable nuclear resonances and the contribution of their decay products to the observed light particle yields. The dashed curve in Figure 12 shows the temperature dependence of the proton cross sections as predicted by their model calculations<sup>19)</sup>, see upper horizontal scale of the figure. In order to make it possible to compare the trends predicted by these calculations to experimental observations, a linear relation was assumed between the upper and lower horizontal scales. This linear relation between  $\ln(T)$  and  $\ln([E - V_C]/T)$  was taken from the measured energy dependence of the moving source temperature parameter  $T$ , as is shown in the insert of Figure 12. The

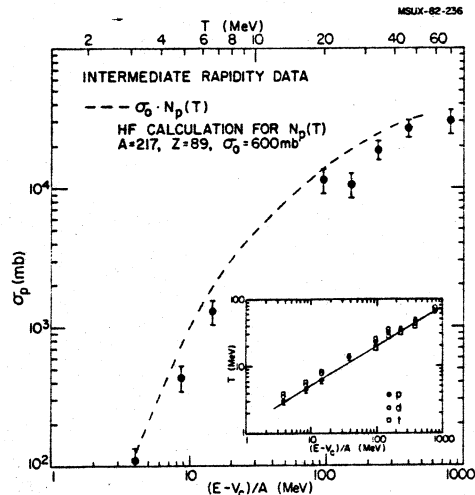


Figure 2: Temperature dependence (upper horizontal scale) of the proton emission cross sections as calculated from Hauser-Feshbach type calculations for the deexcitation of a hot drop of nuclear matter.<sup>18, 19)</sup> The comparison with the experimental data (lower horizontal scale) has been made by assuming the linear relation between  $\ln(T)$  and  $\ln([E - V_c]/A)$  that is shown by the straight line in the insert of the figure. For comparison, the data of Fig. 8 are also reproduced in the insert.

model calculations reproduce the observed energy dependence of the intermediate rapidity proton cross sections rather well. In this picture, the rapid decrease of the proton yield with decreasing temperature (or beam energy) is mainly a consequence of energy conservation: a drop of nuclear matter at high temperature will evaporate more particles to cool down to a stable nucleus than a drop of lower initial temperature.

The composite particle to proton ratios calculated<sup>19)</sup> for the evaporation from a hot liquid drop are shown by the solid curves in Figure 11, where the relation to the experimental data has been established in the same way as for Figure 12. These calculations reproduce the correct magnitudes of the observed particle ratios as well as the weak energy dependence of the  $\sigma_d/\sigma_p$  and  $\sigma_t/\sigma_p$  ratios and the strong energy dependence of the  $\sigma_\alpha/\sigma_p$  ratio.

The qualitative differences of the yield ratios  $\sigma_x/\sigma_p$  predicted by the model of Friedman and Lynch can be rather easily understood in terms of the temperature dependence of the various branching ratios  $\Gamma_x/\Gamma_p$  as given by the approximate expressions of eqs. 8 and 9. The first term appearing in the exponent on the right hand side of eq. 8,  $Q_x/T$ , depends on the exit channel Coulomb barriers,  $V_p$  and  $V_x$ , and on the liquid drop binding energies via the separation energies,  $B_p$  and  $B_x$ . This term determines the branching ratios for small temperatures. For large temperatures it vanishes making the branching ratios independent of the detailed liquid drop properties. The second term appearing in the exponent on the right hand side of eq. 8,  $(A_x - 1)\pi^2 T / 4\epsilon_p$ , depends mainly on the mass number of the emitted particle. This term will determine the branching ratios at higher

temperatures where nucleon emission is strongly favored over the emission of composite particles.

A more quantitative example is given in Figure 13 where the approximate temperature dependence of the branching ratios  $\Gamma_n/\Gamma_p$ ,  $\Gamma_d/\Gamma_p$ ,  $\Gamma_t/\Gamma_p$ , and  $\Gamma_\alpha/\Gamma_p$  has been calculated for a liquid drop with  $A = 217$  and  $Z = 89$ . For simplicity the ratio  $C_n/C_p$  has been set to unity. Using standard liquid drop binding energies and Coulomb barriers<sup>18)</sup>, positive values are obtained for  $Q_n$  and  $Q_\alpha$ . The corresponding values of  $\Gamma_n/\Gamma_p$  and  $\Gamma_\alpha/\Gamma_p$  decrease rapidly with increasing temperature. (Note the large values of  $\Gamma_n/\Gamma_p > 100$  for temperatures below 2 MeV; this reflects the well known fact that heavy compound nuclei of not too high excitation energies decay primarily via neutron emission.) The values of  $Q_d$  and  $Q_t$ , on the other hand, are negative. As a consequence, the  $\Gamma_d/\Gamma_p$  and  $\Gamma_t/\Gamma_p$  ratios exhibit broad maxima as a function of temperature. The main features of the observed composite particle to proton ratios,  $\sigma_x/\sigma_p$ , can be explained in a qualitative way by the temperature dependence of the  $\Gamma_x/\Gamma_p$  ratios of the primary hot liquid drop. As this liquid drop cools by particle emission, these branching ratios will change because of their dependence on temperature, liquid drop binding energy and Coulomb barrier. These effects are, of course, incorporated in the more detailed calculations of Ref.<sup>18)</sup>.

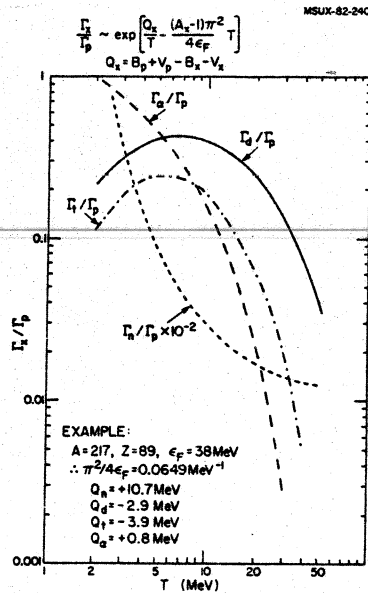


Figure 13: Approximate temperature dependence of the branching ratios  $\Gamma_n/\Gamma_p$ ,  $\Gamma_d/\Gamma_p$ ,  $\Gamma_t/\Gamma_p$ , and  $\Gamma_\alpha/\Gamma_p$  for a hot liquid drop of nuclear matter consisting of  $Z = 89$  protons and  $A - Z = 128$  neutrons.



The variation of  $Q_x$  along the valley of stability is shown in Figure 14. As is evident from the figure the various values of  $Q_x$  vary rather slowly as a function of the liquid drop mass number. As a consequence, the calculated particle ratios should be rather insensitive to the mass of the original hot liquid drop. These expectations have been verified by more detailed computations<sup>18,19</sup>) and add weight to the assumption that particle evaporation from a hot liquid drop of nuclear matter should be included into future theoretical considerations of light particle production at intermediate energies.

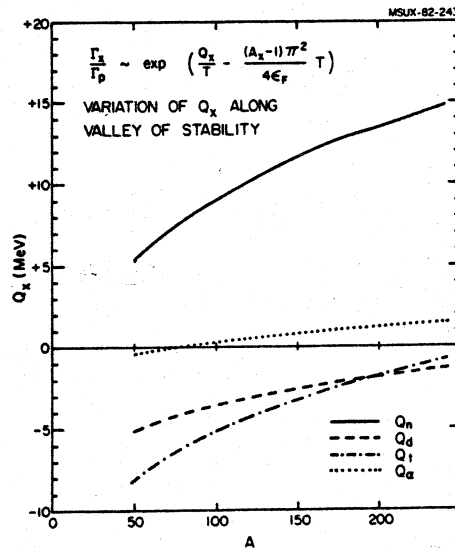


Figure 14: Variation of  $Q_n$ ,  $Q_d$ ,  $Q_t$  and  $Q_\alpha$  along the valley of stability (see eqs. 8 and 9).

#### 4. Summary and Conclusion

In this talk I have outlined some of the characteristic features of intermediate rapidity light particle emission observed over the projectile energy range of  $(E-V_c)/A \approx 4-800$  MeV. In order to reduce contributions from peripheral reactions, small emission angles were excluded from the analysis. Furthermore, low energy regions of the spectra that were obviously dominated by evaporation from the compound nucleus were suppressed in the data analysis. The trends of the data were then discussed in terms of the simple picture of a moving thermal source of nucleons. Most likely, such an approach represents a drastic simplification of a more complex physical reality. On the other hand, it helped to establish some rather general features of the data:

- 1) Rather similar temperature parameters and source velocities are extracted for protons, deuterons, tritons and alpha particles, consistent with the hypothesis of local thermal equilibrium.
- 2) The measured temperature parameters increase smoothly with increasing projectile energy per nucleon above the Coulomb barrier.

The observed energy dependence is rather similar to the one expected for a Fermi gas consisting of comparable numbers of projectile and target nucleons.

3) The proton cross sections rise by more than two orders of magnitude over the energy range of  $(E - V_C)/A = 4-800$  MeV. At lower energies,  $(E - V_C)/A \lesssim 100$  MeV, the observed cross sections exclude an interpretation in terms of a free gas of participant nuclear matter formed in the region of geometrical overlap as expected by the participant spectator model. The energy dependence of the proton cross section can, however, be rather well described in terms of particle evaporation from a hot liquid drop of nuclear matter.

4) Rather large differences are observed in the composite particle to proton yield ratios,  $\sigma_x/\sigma_p$ . The relative yields of protons, deuterons and tritons exhibit no strong energy dependence. The  $\sigma_\alpha/\sigma_p$  ratio, on the other hand, decreased by about  $1\frac{1}{2}$  orders of magnitude between incident energies per nucleon above the Coulomb barrier of about 4 and 800 MeV.

5) The assumption of a free, strongly interacting gas of nuclear matter can reproduce the energy dependence of the  $\sigma_d/\sigma_p$  and  $\sigma_\alpha/\sigma_p$  ratios rather well but fails to explain the energy dependence of the  $\sigma_t/\sigma_p$  ratio. The assumption of evaporation from a hot liquid drop of nuclear matter is in qualitative agreement with the observed light particle yield ratios. In both models the production and decay of particle unstable states has to be included.

In concluding, I would like to express my personal opinion about our present state of knowledge. Present experimental results are consistent with the assumption of the attainment of local thermal equilibrium in nucleus-nucleus collisions at intermediate energies. It should have become apparent that the simple assumption of a free, strongly-interacting gas of nuclear matter cannot explain the experimental observations at incident energies below about 100 MeV per nucleon. This was, of course, expected from our discussion of the liquid and gas phases. The simple model of evaporation from a hot liquid drop of nuclear matter, on the other hand, can explain the global trends of present observations rather well, indicating the relevance of the liquid phase of nuclear matter for projectile energies below, at least, 100 MeV per nucleon. However, the present model has not yet been formulated to include the feature of local thermal equilibrium which the data have ample evidence for. We still lack a good comprehensive model on how a locally heated droplet of nuclear matter forms and decays by the emission of composite particles and nucleons. Even more difficult to answer is the question of whether liquid and gas phases are (temporarily) in equilibrium as would be required for the establishment of the liquid gas phase instability at the critical point. We are certainly making progress. At the same time, we should be aware that a lot of detailed experimental and theoretical work lies ahead of us before we can hope to determine the more interesting properties of hot nuclear matter. Finally, I should like to stress that many of our present concepts will have to be revised as new and better data come along.

#### Acknowledgements

It is a pleasure to thank Dr. W.G. Lynch and Dr. G.D. Westfall for many stimulating discussions and for making their calculations available prior to publication. In addition I should like to express my gratitude to my colleagues over the last few years for their enthusiastic support of this research program during experiments, data analysis and discussions: N. Anantaraman, T.C. Awes, B.B. Back, H. Breuer, G.M. Crawley, M.V. Curtin, R.E. Ellis, A. Galonsky, B. Glagola, B. Hasselquist, B.V. Jacak, J. Kasagi, R.L. Legrain, W.G. Lynch, T.J. Majors, M.J. Murphy, G. Poggi, L.W. Richardson, S. Saini, D.K. Scott, T.J.M. Symons, M.B. Tsang, V.E. Viola, Jr., R.E. Warner, G.D. Westfall, and K.L. Wolf.

This material is based upon work supported by the National Science Foundation under Grant No. PHY 80-17605.

#### References

- 1) W. Hauser and H. Feshbach, Phys. Rev. 87 (1952) 366.
- 2) A.Z. Mekjian, Phys. Rev. C17 (1978) 1051.
- 3) J.I. Kapusta, Phys. Rev. C16 (1977) 1493.
- 4) J. Gosset, J.I. Kapusta, and G.D. Westfall, Phys. Rev. C18 (1978) 844.
- 5) G. Röpke, L. Münchow, and H. Schulz, Phys. Lett. B110 (1982) 21 and Nucl. Phys. A379 (1982) 536.
- 6) M.W. Curtin, H. Toki, and D.K. Scott, Michigan State University Preprint, MSUCL-373, 1982.
- 7) H. Schulz, L. Münchow, G. Röpke, and M. Schmidt, Niels Bohr Institute Preprint, NBI-82-10, 1982.
- 8) J. Kasagi, S. Saini, T.C. Awes, A. Galonsky, C.K. Gelbke, G. Poggi, D.K. Scott, K.L. Wolf, and R.L. Legrain, Phys. Lett. 104B (1981) 434.
- 9) T.C. Awes, G. Poggi, C.K. Gelbke, B.B. Back, B.G. Glagola, H. Breuer and V.E. Viola, Jr., Phys. Rev. C24 (1981) 89.
- 10) B.B. Back, K.L. Wolf, A.C. Mignerey, C.K. Gelbke, T.C. Awes, H. Breuer, V.E. Viola, Jr., and P. Dyer, Phys. Rev. C22 (1980) 1927.
- 11) R.L. Auble, J.B. Ball, F.E. Bertrand, C.B. Fulmer, D.C. Hensley, I.Y. Lee, R.L. Robinson, P.H. Stelson, D.L. Hendrie, H.D. Holmgren, J.D. Silk, and H. Breuer, Phys. Rev. Lett. 49 (1982) 441.
- 12) G.D. Westfall, B.V. Jacak, N. Anantaraman, M.V. Curtin, G.M. Crawley, C.K. Gelbke, B. Hasselquist, W.G. Lynch, D.K. Scott, M.B. Tsang, M.J. Murphy, T.J.M. Symons, R. Legrain, and T.J. Majors, Phys. Lett. B.
- 13) T.C. Awes, S. Saini, G. Poggi, C.K. Gelbke, D. Cha, R. Legrain, and G.D. Westfall, Phys. Rev. C25 (1982) 2361.
- 14) W.G. Lynch, L.W. Richardson, M.B. Tsang, R.E. Ellis, C.K. Gelbke, and R.E. Warner, Phys. Lett. 108B (1982) 274.
- 15) G.D. Westfall, J. Gosset, P.J. Johansen, A.M. Poskanzer, W.G. Meyer, H.H. Gutbrod, A. Sandoval, and R. Stock, Phys. Rev. Lett. 37 (1976) 1202.
- 16) J. Gosset, H.H. Gutbrod, W.G. Meyer, A.M. Poskanzer, A. Sandoval, R. Stock, and G.D. Westfall, Phys. Rev. C16 (1977) 629.
- 17) G.D. Westfall, private communication.
- 18) W. Friedman and W.G. Lynch, to be published.
- 19) W.G. Lynch, private communication.